Supplementary Material Available: Tables IX-XI, calculated Cartesian coordinates, moments of inertia, and vibrational frequencies of norbornene (**1**), norbornane (**2**), and norbornadiene (**3**) (6 pages). Ordering information is given on any current masthead page.

References and Notes

(1) For part 43, see M. J. S. Dewar and D. Landman, *J. Am. Chem. Soc.*, **99**, 6179 (1977).
(2) Robert A. Welch Postdoctoral Fellow.
(3) G. Herzberg, "Molecular Spectra and Molecular Structure", Vol. 2, Van Nostrand, Princeton, N.J., 1945, Chapter V; G. N. Lewis and M. Randall, "Thermodynamics", K. S. Pitzer and L. Brewer, Ed., McGraw-Hill, New York, N.Y., 1961, Chapter 27.
(4) R. C. Bingham, M. J. S. Dewar, and D. H. Lo, *J. Am. Chem. Soc.*, **97**, 1285, 1294, 1302, 1307 (1975); M. J. S. Dewar, D. H. Lo, and C. A. Ramsden, *ibid.*, **97**, 1311 (1975).
(5) M. J. S. Dewar, *Chem. Br.*, **11**, 97 (1975); *Discuss. Faraday Soc.*, **62**, 197 (1977).
(6) M. J. S. Dewar and G. P. Ford, *J. Am. Chem. Soc.*, **99**, 1685 (1977).
(7) M. J. S. Dewar and G. P. Ford, *J. Am. Chem. Soc.*; in press.
(8) M. J. S. Dewar and H. S. Rzepa, *J. Am. Chem. Soc.*, submitted for publication.
(9) MINDO/3 geometries for compounds not previously published follow: $CH_2{=}N^+{=}N^-$ NN = 1.113; CN = 1.274; CH = 1.113; HCH = 115.1; lit.[10] NN = 1.139; CN = 1.300; CH = 1.077; HCH = 126.1°.

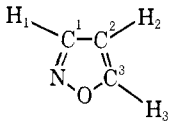

NO = 1.368; NC^1 = 1.312; C^1C^2 = 1.445; C^2C^3 = 1.371; CO = 1.323; H^1C^1 = 1.106; H^2C^2 = 1.095; H^3C^3 = 1.106; C^3ON = 110.57°; ONC^1 = 106.71°; NC^1C^2 = 109.93°; $C^1C^2C^3$ = 107.44°; C^2C^3O = 105.35°; $H^1C^1C^2$ = 126.77°; $H^2C^2C^3$ = 128.83°; $H^3C^3C^2$ = 133.78.
(10) I. Sheridan, *Adv. Mol. Spectrosc., Proc. Int. Meet., 4th*, 1 (1962).
(11) A. Rogstad, P. Klaboe, H. Baranska, E. Bjarnov, D. H. Christensen, F. Nicolaisen, O. F. Nielsen, B. N. Oyvrin, and S. J. Oyvrin, *J. Mol. Struct.*, **20**, 403 (1974).
(12) H. W. Wooley, *J. Res. Natl. Bur. Stand.*, **56**, 105 (1956).
(13) R. S. McDowell, *J. Chem. Phys.*, **39**, 526 (1963).
(14) R. E. Pennington and K. A. Kobe, *J. Chem. Phys.*, **22**, 1442 (1954).
(15) R. S. McDowell and F. H. Kruse, *J. Chem. Eng. Data*, **8**, 547 (1963).
(16) (a) M. J. S. Dewar and S. Kirschner, *J. Chem. Soc., Chem. Commun.*, 463 (1975); (b) M. J. S. Dewar, G. P. Ford, and H. S. Rzepa, *ibid.*, submitted; (c) M. J. S. Dewar and S. Kirschner, *J. Am. Chem. Soc.*, **96**, 6809 (1974); (d) M. J. S. Dewar and S. Kirschner, *J. Chem. Soc., Chem. Commun.*, 461 (1975); (e) M. J. S. Dewar, G. P. Ford, M. L. McKee, H. S. Rzepa, and L. E. Wade, *J. Am. Chem. Soc.*, **99**, 5069 (1977).
(17) D. M. Golden and J. I. Brauman, *Trans. Faraday Soc.*, **65**, 464 (1969).
(18) M. J. S. Dewar and Y. Yamaguchi, unpublished work.
(19) "JANAF Thermochemical Tables", Dow Chemical Co., Midland, Mch., 1965.
(20) V. T. Aleksanyan and Kh. E. Sterin, *Mater. Desyatigo Vses. Soveshch. Spectrosk., 1957, L'vor Gosudurst. Univ. im. I. Franko, Fiz. Sbornik 1*, **No. 3**, 59; *Chem. Abstr.*, **53**, 21158*a* (1959).
(21) J. F. Chiang and R. Chiang, Abstracts, 168th National Meeting of the American Chemical Society, Atlantic City, N.J., Sept. 1974.
(22) R. Walsh and J. M. Wells, *J. Chem. Thermodyn.*, **8**, 55 (1976).
(23) R. Walsh and J. M. Wells, *J. Chem. Thermodyn.*, **7**, 149 (i975).
(24) R. M. Joshi, *J. Polym. Sci., Part A-2*, **8**, 679 (1970).
(25) R. H. Boyd, S. N. Sanwal, S. Shary-Tehrany, and D. McNally, *J. Phys. Chem.*, **75**, 1264 (1971).
(26) H. E. O'Neal and S. W. Benson, *J. Chem. Eng. Data*, **15**, 266 (i970).

Dissociative Pathways and Molecular Vibrations. Compliance Constants and Minimum Energy Coordinates for BF_3 and SO_3

B. I. Swanson,* J. J. Rafalko, H. S. Rzepa, and M. J. S. Dewar

Contribution from the Department of Chemistry, University of Texas at Austin, Austin, Texas 78712.

Received April 1, 1977

Abstract: The minimum energy paths for unimolecular dissociation of SO_3 and BF_3 have been probed using vibrational spectroscopy and the semiempirical SCF-MO scheme MNDO. Minimum energy coordinates obtained from spectroscopic data show that initially the minimum energy pathway (MEP) is heterolytic in character, leading to BF_2^+ and SO_2^+ products. Since the thermodynamically favored products are radicals, this information suggests that the MEP must assume covalent character after the initial distortion. A constrained MEP for BF_3, as evaluated using the MNDO SCF-MO method, closely parallels the vibrational minimum energy coordinate out to 0.25 Å distortion of a B-F bond. At greater extensions, inclusion of configuration interaction in the MNDO calculations, or use of the UHF approach, reveals the increasing contribution of an excited covalent electronic configuration to the wave function. This avoided crossing eventually leads to homolytic bond cleavage. Implications concerning the use of minimum energy coordinates as a model of dissociative pathways are discussed.

Introduction

Chemists interested in studying bonding phenomena using vibrational spectroscopy generally model molecular vibrations in terms of displacement coordinates and the Wilson GF formalism.[1] In spite of the wide usage that the GF method has enjoyed, there are difficulties in using force constants as probes of interatomic forces. The value of a force constant is dependent on the coordinate set used to describe the molecule and the force matrix is indeterminant when there are redundancies among the internal coordinates.[2,3] While these mathematical difficulties do not interfere with many aspects of a vibrational study, they are troublesome when it comes to using force constants as bonding parameters. We have been interested in exploring the utility of the alternative compliance constant method,[2-4] which does not have these difficulties.

One of the appealing aspects of the compliant formalism is the direct connection between compliance constants and the reaction coordinate for unimolecular dissociation via minimum energy coordinates[5,6]

$$\mathcal{R}_i = r_i + \sum_{\substack{j=1 \\ \neq i}}^{n} (j)_i r_j = r_i + \sum_{\substack{j=1 \\ \neq i}}^{n} (C_{ij}/C_{ii}) r_j \qquad (1)$$

Here $\{r_i\}$ are unit vectors along the internal coordinate directions, $\{(j)_i\}$ are interaction displacement coordinates,[7] C_{ij} are valence compliance constants, and n gives the number of internal coordinates.

The interest in a tie between reaction pathways and potential functions is by no means new. Linnett and Wheatley[8] and Mills[9] had devised approximate force fields based on the apparent relationship between the signs of the interaction force constants and the geometry change expected upon dissociation.

Table I. The Evaluation of $(R_2)_{R_1}$ and $(\alpha_{23})_{R_1}$ for BF_3 Using MNDO

ΔR_1, Å	R_2, Å	α_{23}, deg[a]	$(R_2)_{R_1}$[b]	$(\alpha_{23})_{R_1}$, deg/Å[b]
0.0	1.316	120.0		
0.014	1.314 53	120.385 84	−0.1050	27.56
0.019	1.314 05	120.520 66	−0.1026	27.40
0.024	1.313 54	120.653 52	−0.1025	27.23
0.029	1.313 05	i20.785 58	−0.1017	27.09
0.034	1.312 56	120.917 06	−0.1012	26.97
0.039	1.312 07	121.047 86	−0.1008	26.87
0.049	1.311 19	121.320 70	−0.098 16	26.95
0.059	1.310 23	121.576 20	−0.097 80	26.70
0.084	1.307 87	122.195 68	−0.096 79	26.02
0.109	1.305 74	122.801 88	−0.094 13	25.71
0.134	1.303 73	123.402 88	−0.091 57	25.39
0.184	1.300 01	124.564 72	−0.086 90	24.81
0.234	1.296 67	125.670 06	−0.082 61	24.23
Polynomial fit of MNDO data[c]			−0.103	26.8
Spectroscopic calculation			−0.1074	23.4

[a] α_{23} is the angle formed by R_2 and R_3. [b] These interaction coordinates were calculated by dividing the total change from equilibrium of R_2 or α_{23} by the total change in R_1. $(R_1)\alpha_{23}$ and $(R_2)\alpha_{23}$ have also been determined from MNDO by observing the response of the geometry to the angle change in α_{23}. At a 2° distortion of α_{23}, $(R_1)\alpha_{23}$ = 0.063 Å/rad and $(R_2)\alpha_{23}$ = −0.023 Å/rad. The corresponding values from the spectroscopic calculations are 0.075 and −0.037 Å/rad, respectively. [c] These values were obtained from a least-squares fit of the data to a polynomial of order 3.

More recently Machida and Overend[5] and Jones and Ryan[10] have further developed this relationship between potential constants and geometry changes. Recently, we have shown that minimum energy coordinates provide the best measure of the minimum energy path for unimolecular dissociation or intramolecular rearrangement in the quadratic limit.[6]

The path $\mathcal{R}_i$ is defined by minimizing the potential energy with respect to all internal coordinates R_j following a fixed distortion in R_i. Accordingly, $\mathcal{R}_i$ is a constrained pathway; the MEP is best defined by minimizing potential energy with respect to a unit distortion in internal coordinate space with no constraints on any one internal coordinate.[11] The difference between $\mathcal{R}_i$ and the unconstrained MEP will be greatest at infinitesimal distortions from the equilibrium configuration, where the unconstrained MEP will follow that normal mode with the lowest force constant. The linear path given by $\mathcal{R}_i$ represents a linear combination of normal modes. For example, in dissociation of CO_2 the unconstrained MEP will initially follow the asymmetric stretch, $Q_3 = 1/\sqrt{2}(R_1 - R_2)$, while $\mathcal{R}_{CO}$ involves both Q_3 and the symmetric stretch, $Q_1 = 1/\sqrt{2}(R_1 + R_2)$. The discrepancy between $\mathcal{R}_i$ and the unconstrained MEP is severe near equilibrium. However, it should be noted that $\mathcal{R}_i$ provides a much more realistic approximation to the unconstrained MEP at larger than infinitesimal distortions, where modes of different symmetry will contribute to the MEP. In principle, any normal mode which transforms as the totally symmetric representation in the point group of the distorted molecule may contribute to the MEP. Dissociation of CO_2 provides a striking example of this mixing of normal modes as the overall compression of the C-O bond length in proceeding from CO_2 to CO is quite small (ΔR = −0.04 Å; for CO_2 $\mathcal{R}_{CO_1} = r_1 - 0.078r_2$). While the unconstrained MEP will follow one normal mode in the initial distortion from equilibrium, curvature will force this MEP to eventually cross $\mathcal{R}_i$ at larger distortions. It should also be noted that the evaluation of an unconstrained MEP via SCF-MO methods is nontrivial and a constrained approach is generally used.[11]

Our principal interest now is to determine whether or not compliance constants, determined uniquely from vibrational data, provide any new chemically meaningful information concerning reaction pathways. In a study of the unique compliance functions for some four- and six-coordinate complexes[12] we were able to show that the minimum energy coordinates agree remarkably well with that structural change which occurs upon dissociation. In the present study we have extended this method to the trigonal planar systems SO_3 and BF_3. In order to compare the minimum energy coordinate with that structural change expected from MO theory, a similarly constrained MEP for BF_3 has been evaluated using SCF-MO calculations. In this paper subsequent reference to the MEP will imply this constained pathway.

Results

MO Calculations for BF_3. A. Small Extensions of the B-F Bond. The molecular orbital calculations were carried out using a newly developed semiempirical method based on the NDDO approximation, which we have called MNDO (modified neglect of diatomic overlap).[13] The method differs from MINDO/3 in the retention of a large number of two-center two-electron repulsion integrals and two-center core electron attraction terms. It has resulted in a considerable quantitative improvement in calculated geometries, heats of formation, and other properties of the second-period elements, particularly boron and fluorine.[14] The potential surface for dissociation was investigated by constraining one B-F distance to a series of values and minimizing the energy with respect to all other coordinates at these values. Even though an overall C_s symmetry was maintained as one B-F bond was stretched, the distortion from planarity was negligible. An extended CI with the inclusion of ten excited state configurations had little effect on the energy of the system up to a bond distortion of 0.23 Å.[15] The response of the geometric parameters is presented in Table I as a function of the change in R_1.

B. Complete Dissociation of the B-F Bond. At B-F extensions of greater than 1.7 Å a significant contribution from a single excited a_1 configuration to the ground-state wave function was found. The molecule was studied from a B-F distance of 1.5 Å to complete dissociation (2.5 Å) using a CI based primarily on this configuration. A continuous pathway was found, with the system remaining planar throughout. The constrained MEP is illustrated in Figure 1. Also included are results obtained using an unrestricted Hartree-Fock approach such as described by Salotto and Burnelle[16] for the study of dissociation reactions, and recently applied in an MNDO study of the dissociation of ozone.[17]

The agreement between the UHF and CI approaches is only qualitative; better quantitative agreement would probably be obtained by using a larger number of configurations in the CI method and projecting the contaminant triplet and higher spin

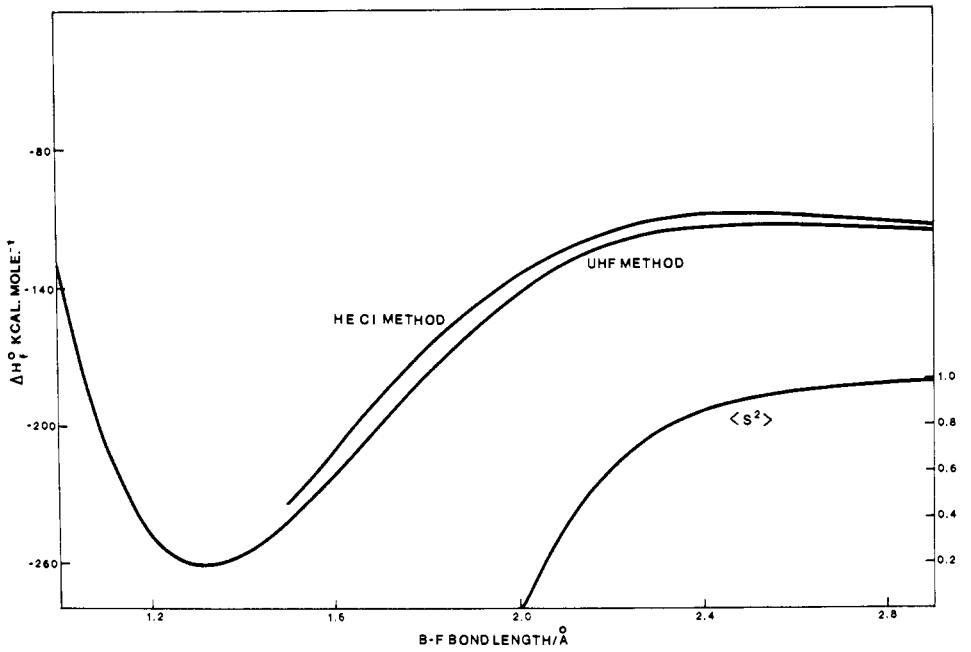

Figure 1. Calculated energy vs. B–F bond length for the dissociation of BF_3. HE CI and UHF refer to the half electron CI method and the S_0 unrestricted Hartree–Fock method, respectively. $\langle S^2 \rangle$ represents the expectation value of the operator S^2 obtained for the UHF wave function.

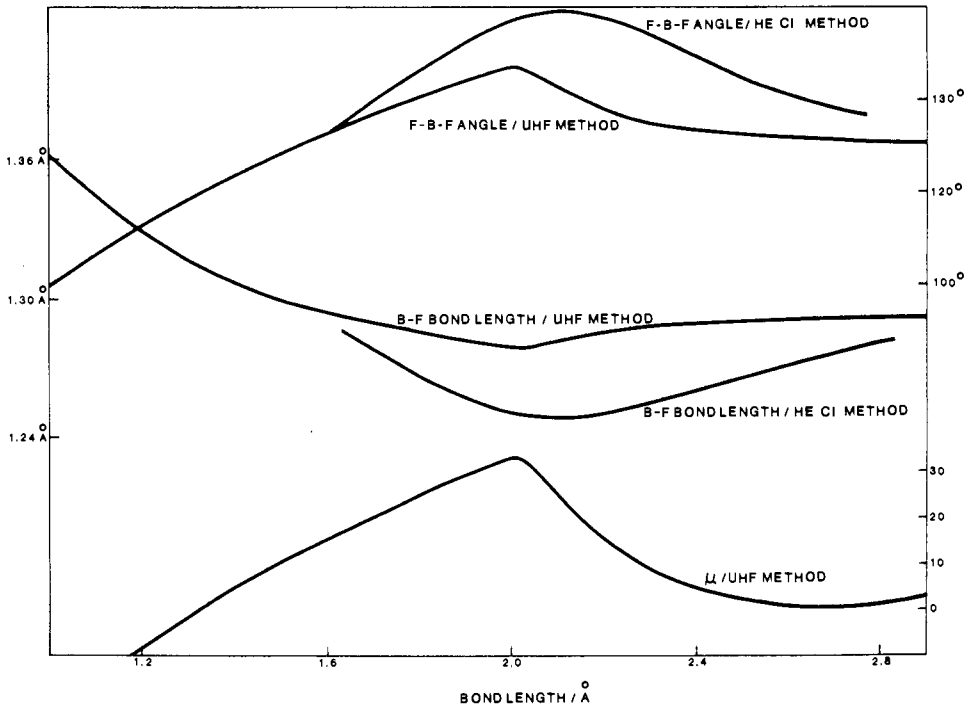

Figure 2. Calculated response in geometrical parameters and dipole moment for the dissociation of BF_3 into BF_2· and F·.

states from the UHF wave function. The discontinuities apparent in the geometrical responses in the region $R_{B-F} = 2.0$ Å (Figure 2) using the UHF method are probably an artifact, the RHF + CI method showing more continuous behavior. The qualitative trends predicted by *both* methods that we wish to emphasize are the large increase in the F-B-F angle to a maximum, followed by a *decrease* to a final value of about 126°. Similarly, the B–F bond length is predicted to decrease to a minimum, followed by an increase to about 1.29 Å in BF_2. The significance of these nonmonotonic responses in the geometry will be discussed later.

General Vibrational Refinements. The symmetry coordinates for an AX_3 planar molecule have been described elsewhere.[18] The compliance constants were calculated with the program COMPLY.[19] The frequency data, Coriolis constants, and mean amplitudes of vibration were refined simultaneously. Each data type was given equal importance in determining the compliant field. The frequencies were weighted by the equation $w_i = \nu_i^6/(\sigma(\nu_i))^2$, where ν_i is the frequency of the normal mode Q_i and $\sigma(\nu_i)$ is the estimated error in the observed frequency. The weights for the Coriolis constants were set equal to $1/(\sigma(\zeta_i))^2$ where $\sigma(\zeta_i)$ is the estimated error of the observed ζ constant i. Mean-square amplitudes, which were only included in the refinements of BF_3,[20] were weighted as $0.05/\Sigma_i(\sigma_i)^2$. Here

Table II. Frequency Data

Assignment	SO_3[a]			BF_3[e]	
	A[b]	B[c]	C[d]	^{10}B[f]	^{11}B[f]
A_1', ν_1	1068	1048.1	1064.9	903.6	903.6
E', ν_3	1389.9	1409.0	1410.0	1512.2	1460.2
E', ν_4	532.2	538.6	535.6	488.7	487.0

[a] Reference 18. Three refinements were undertaken using frequency sets A, B, and C in order to establish an error range for the potential constants. Their solutions are listed in Table III. [b] Observed frequencies. [c] Calculated harmonic frequencies obtained for a valence force model. See *a*. [d] Calculated harmonic frequencies obtained by including some estimated cubic interaction force constants in the valence force model. See *a*. [e] Reference 21. [f] Harmonic frequencies.

Σ_i is the mean-square amplitude and σ_i is the standard error in the root mean square amplitude.

The frequency data for the A_1' and E' symmetry blocks for SO_3 and BF_3 are listed in Table II. We feel that these are the best measurements to date. Harmonic frequencies were selected when they were available. Unfortunately, there are some discrepancies in the reported values of some of the ζ constants. The reliability of the resulting compliants using the above data will be appraised along with the differences between the observed and calculated observables in latter sections dealing with the individual molecules.

SO_3. Lack of sufficient data has prevented the complete evaluation of the anharmonicity corrections for SO_3. However, Dorney et al.[18] have estimated harmonic frequencies from two force field models. In order to establish an error range associated with the potential function, the observed frequencies and the two sets of calculated frequencies were refined separately with ζ_3. The three compliance functions so obtained are presented in Table III. Two independent groups have measured ζ_3 by band contour[22] and fine structure methods.[22,23] Their findings were within experimental error of each other. The fine structure value of 0.474 ± 0.04[22] was used in the refinements.

For both A_1' and E' blocks the number of unique compliants is equivalent to the number of observables. This equality precludes the direct determination of errors from a least-squares method. For C_{11}, C_{33}, and C_{44}, the errors were taken as the largest difference between the anharmonic constants (solution A, Table III, obtained from the observed frequencies) and the corresponding constants from the two sets of calculated frequencies (B, C). C_{34} is relatively insensitive to these different frequency sets, but it is quite dependent on the value of the ζ constant. The error in C_{34} was estimated from two additional refinements of the observed frequencies (A) with a ζ_3 which had been adjusted to cover the range of its uncertainties. These two solutions are presented in the lower portion of Table III and they are labeled according to the value of the ζ constant used in the refinement. The error in C_{34} was taken as the largest difference between C_{34} of A and the C_{34}'s from the solutions in which the ζ constant was varied over its known experimental uncertainty. The errors are listed in parentheses after the compliance constants and interaction constants for solution A of Table III. These errors provide a range of confidence.

BF_3. High-[24-26] and low-[27,28] resolution infrared techniques have been used to determine the Coriolis constants for BF_3. Unfortunately, the two methods yield vastly different values. The band contour method of Edgell and Moynihan[29] consistently gave lower values than those obtained from partially resolved spectra. Duncan[24] and Dreska et al.[30] have previously discussed this problem. Even though the high-resolution data are preferred, both sets of Coriolis constants were refined and their solutions and input ζ's are presented in Table IV.

A clear choice of the best solution can be made on the basis of the MNDO calculations. The molecular orbital value of $(\alpha_{23})_{R_1} = 0.468$ rad/Å supports the first solution in Table IV resulting from the high-resolution Coriolis constants. In addition, the data fit is much better for this solution than the second. The average errors are 0.3 cm^{-1} for the frequencies, 0.3% in the ζ constants, and 8% in the amplitudes of vibration.

Discussion

The general quadratic compliance function for BF_3 is uniquely determined by the spectroscopic data. The inclusion of Coriolis data[24,25] in the least-squares estimate of compliants fixes the value of the off-diagonal E' symmetry compliant. Accordingly, the interaction displacement coordinates and the minimum energy coordinates for BF_3 are well determined.

In this report we are primarily concerned with the question of how well minimum energy coordinates model the MEP for unimolecular dissociation. A useful comparison in this regard is that of $\mathcal{R}_{BF}$ and the overall structural change which accompanies dissociation. In the case of BF_3 unimolecular dissociation most certainly proceeds via homolytic cleavage of the B-F bond, since the radical species BF_2 + F are thermodynamically favored over the formation of ionic species.[31] The structure of BF_2 has not been determined experimentally. The MNDO results predict a bond length of 1.29 Å and an angle of 125.6°, suggesting a slight decrease in the bond length and increase in the angle compared with BF_3. This is in accord with trends expected from valence shell electron pair repulsion theory (VSEPR), where the assumption is that the unpaired electron in BF_2 will not repel the fluorine atoms as strongly as those electrons involved in a B-F bond.

The minimum energy coordinate corresponding to unimolecular dissociation

$$\mathcal{R}_{BF_1} = \mathbf{R}_1 - 0.107(\mathbf{R}_2 + \mathbf{R}_3) + 0.406\alpha_{23} - 0.203(\alpha_{12} + \alpha_{13})$$

is in agreement with the expected structural change as regards the direction of the angle and bond length responses. However, the magnitudes of the changes indicated by $\mathcal{R}_{BF_1}$ are large relative to the overall change expected on the basis of homolytic cleavage of $B-F_1$ (above). The angle response taken alone ($(\alpha_{23})_{R_1} = 23.8°/Å$) suggests ion rather than radical formation since BF_2^+ is calculated by MNDO to be linear.[14]

There are insufficient vibrational data for SO_3 to allow a unique determination of $C_{R_1R_2}$ and the interaction displacement coordinate $(R_2)_{R_1}$. The available data indicate that $C_{R_1R_2}$ and $(R_2)_{R_1}$ are essentially zero. The interaction constant $C_{R_1\alpha_{23}}$ is, however, well determined from the Coriolis data. The corresponding interaction coordinate, $(\alpha_{23})_{R_1} = 13.8°/Å$, indicates that the SO_2 fragment opens up as $S-O_1$ is stretched.

As was the case for BF_3, homolytic cleavage and the subsequent formation of SO_2 and O is expected for dissociation on the basis of thermodynamic data.[31] However, there is an ambiguity concerning whether singlet SO_2 and singlet O, or triplet SO_2 and O, are formed. The structural response indicated by $\mathcal{R}_{SO_1}$ opposes the overall structural change in forming singlet SO_2 (O-S-O ∠ = 119.5° [32]). The direction of the angle change given by $\mathcal{R}_{SO_1}$ is in agreement with formation of triplet SO_2 (for the $^3B_1$ state of SO_2 the O-S-O ∠ = 126.2° [33]). However, the initial dissociative pathway as modeled by $\mathcal{R}_{SO_1}$ looks more like what would be expected if SO_2^+ and O^- were formed rather than the favored neutral species. The structure of the SO_2^+ fragment formed upon dissociation may be crudely estimated assuming that the path $\mathcal{R}_{SO_1}$ is followed and that the $S-O_1$ bond is broken at the S-O van der Waals distance.

Table III. Symmetry Compliance Constants and Interaction Coordinates for SO_3

Frequency data set[a]	C_{11}[b]	C_{33}	C_{44}	C_{34}	$(\alpha_{23})_{R_1}$[d]	$(R_2)_{R_1}$[d]
A	0.0930 (36)[c]	0.0964 (31)	0.823 (30)	0.035 (14)	0.24 (10)	−0.012 (27)
B	0.0966	0.0938	0.797	0.034	0.23	0.010
C	0.0936	0.0936	0.806	0.033	0.24	0.00
ζ_3^e 0.514		0.0973	0.801	0.021		
ζ_3^e 0.434		0.0960	0.832	0.048		

[a] See Table II and text for origin. [b] Units are Å mdyn^{-1} for C_{11} and C_{33}, rad^2 Å^{-1} mdyn^{-1} for C_{44}, rad mdyn^{-1} for C_{34}, and rad Å^{-1} for $(\alpha_{23})_{R_1}$. [c] Errors are in units of the last digit of each entry. See text for explanation. [d] The interaction coordinates were obtained from the following relation: $C_{11} = C_{R_1R_1} + 2C_{R_1R_2}$, $C_{33} = C_{R_1R_1} - C_{R_1R_2}$, $C_{34} = C_{R_1\alpha_{23}} - C_{R_i\alpha_{12}}$, and $0.0 = C_{R_1\alpha_{23}} + 2C_{R_1\alpha_{12}}$. $C_{R_1\alpha_{12}}$ represents the interaction between a bond stretch with an adjacent angle. $C_{R_1\alpha_{23}}$ describes the interaction between a bond stretch and an angle that does not include the stretching coordinate. [e] These two solutions were obtained by refining the observed frequencies with the listed ζ constants which have been amended by ±0.04.

In effect, the difference between the van der Waals distance for S-O and the equilibrium S-O distance in SO_3 is used as the multiplicative factor to estimate the overall structural rearrangement. Using this approach the estimated O-S-O angle in the SO_2^+ fragment is 144°. This agrees favorably with the angle, 137°, of the ($^2A_1$) state of SO_2^+ which has been estimated from the photoelectron spectra of SO_2.[34] The predicted value of 144° is also quite reasonable for an AB_2 system with one stereochemically active electron. For example, in going from NO_2^- to NO_2 the corresponding increase in the O-N-O angle is ca. 19°.[35] Essentially, the SO_2^+ structure predicted assuming that SO_3 dissociation proceeds heterolytically along $\mathcal{R}_{SO}$ is reasonable.

The minimum energy coordinates obtained from vibrational data and the known structural changes point to interesting dissociative pathways for these two planar AB_3 molecules. The minimum energy coordinates provide information about the initial part of the dissociation while known structures of fragments formed upon dissociation provide a point at the end of the dissociative pathway. Irrespective of whether singlet or triplet SO_2 is formed, the striking difference in the initial and final parts of the dissociative pathway (as regards the O-S-O angle) is indicative of a dramatic change in the nature of the MEP from ionic to covalent.

This is best illustrated by the dissociative pathway for BF_3 calculated using MNDO (Figures 1 and 2). The calculated dissociation energy for radical formation (143 kcal/mol) compares well with the experimental value of 151 kcal/mol.[14] Up to a B-F bond length of about 1.7 Å, the wave function is essentially ionic with considerable charge separation, and a comparison of the interaction constants calculated from the MO results with spectroscopic values (Table I) shows excellent agreement up to a B-F distortion of 0.25 Å. For B-F bond lengths of >1.9 Å, the ground state wave function gradually assumes covalent character as a result of an avoided crossing with an excited state of the same symmetry, and the MO pathway is forced from the ionic path projected by the quadratic compliance function. While we have no information concerning the dissociative pathway for SO_3 at intermediate distortions, the minimum energy coordinate $\mathcal{R}_{SO}$ and the structures of the thermodynamically favored products, singlet or triplet SO_2, are indicative of a similar avoided crossing of an ionic ground state with a covalent excited state configuration. Initially, dissociation is accompanied by a significant charge separation and an opening of the O-S-O angle in the SO_2 fragment. At intermediate distortions the flow of electron density is reversed as the covalent configuration begins to dominate the wave function resulting in a decrease of the O-S-O angle.

The present work illustrates that compliance constants and minimum energy coordinates can provide new information about dissociative pathways—information that is difficult to obtain from other sources. Minimum energy coordinates model the structural changes which occur during the initial stages of dissociation. The structure(s) of the thermodynamically favored products, if they are known as in the case of dissociation of SO_3, provide a reference point at the product end of the MEP. Taken together, the product geometry and $\mathcal{R}$ provide insight into the curvilinear nature of the MEP, which may in turn be tied to the changes in the molecular electronic structure which accompany dissociation. In the case of BF_3 we have been able to correctly model those aspects of the MEP obtained from vibrational and structural data using an SCF-MO approach. The implication here is that the MNDO approach provides a good qualitative estimate of the MEP at intermediate distortions, and hopefully also clarifies the nature of the change in molecular electronic structure which accompanies dissociation. Ultimately, this is the sort of information which is needed before we can hope to selectively effect a chemical reaction using the least amount of energy, one of the goals of the emerging area of laser chemistry.

Table IV. Symmetry Compliance Constants and Interaction Coordinates for BF_3

	I[a]	II[a]
C_{11}[b]	0.1094 (3)[c]	0.1094 (17)
C_{33}	0.1543 (3)	0.1525 (14)
C_{44}	1.144 (6)	1.35 (4)
C_{34}	0.08525 (90)	0.1934 (46)
$(\alpha_{23})_{R_1}$	0.408 (6)	0.933 (45)
$(R_2)_{R_1}$	−0.1074 (10)	−0.1040 (51)
$\zeta_3(^{10}B)$	0.810 ± 0.02[d]	0.70 ± 0.04[f]
$\zeta_4(^{10}B)$	−0.809 ± 0.02[e]	
$\zeta_3(^{11}B)$	0.795 ± 0.02[d]	0.64 ± 0.03[f]
$\zeta_4(^{11}B)$	−0.798 ± 0.02[d]	−0.66 ± 0.03[f]

[a] Solutions I and II were obtained from refinements which included the harmonic frequencies from Table II, the mean-squared amplitudes for ^{11}B ($\Sigma_{B\text{-}F}$, 1.58 × 10^{-3} Å^2; $\Sigma_{F\text{-}F}$, 2.93 × 10^{-3} Å^2), and the two sets of ζ constants listed in the lower portion of the table. [b] Units are given in Table III. [c] Numbers in parentheses are standard deviations in units of the last digit. [d] Reference 24. [e] Reference 25. [f] Reference 26.

Acknowledgments. This work was supported by the Air Force Office of Scientific Research (Grant AFOSR 75-2749) and the Robert A. Welch Foundation (Grants F-126 and F-620). The calculations were carried out using the CDC 6400/6600 computer at the University of Texas Computation Center. One of us (H.S.R.) thanks the Science Research Council (U.K.) for the award of a NATO Postdoctoral Fellowship.

References and Notes

(1) E. B. Wilson, Jr., *J. Chem. Phys.*, **7**, 1047 (1939).
(2) J. C. Decius, *J. Chem. Phys.*, **38**, 241 (1963).
(3) L. H. Jones, Proceedings of the 13th International Conference on Coordination Chemistry, Crakow and Zakopane, Poland, Sept 1970.
(4) L. H. Jones and B. I. Swanson, *Acc. Chem. Res.*, **9**, 128 (1976).
(5) K. Machida and J. Overend, *J. Chem. Phys.*, **50**, 4437 (1969).
(6) B. I. Swanson, *J. Am. Chem. Soc.*, **98**, 3067 (1976).
(7) L. H. Jones, *Coord. Chem. Rev.*, 1, 351 (1966).
(8) J. W. Linnett and P. J. Wheatley, *Trans. Faraday Soc.*, **45**, 33, 39 (1949).
(9) I. M. Mills, *Spectrochim. Acta*, **19**, 1585 (1963).
(10) L. H. Jones and R. R. Ryan, *J. Chem. Phys.*, **52**, 2003 (1970).
(11) (a) E. A. McCullough and D. M. Silver, *J. Chem. Phys.*, **62**, 4050 (1975); (b) N. M. Witriol, J. D. Stettler, M. A. Ratner, J. R. Sabin, and S. B. Trickey, *ibid.*, **66**, 1141 (1977).
(12) B. I. Swanson and S. K. Satija, *J. Am. Chem. Soc.*, **99**, 987 (1977).
(13) M. J. S. Dewar and W. Thiel, *J. Am. Chem. Soc.*, **99**, 4899, 4907 (1977).
(14) (a) M. J. S. Dewar and H. S. Rzepa, *J. Am. Chem. Soc.*, to be published; (b) M. J. S. Dewar and M. L. McKee, *ibid.*, **99**, 5231 (1977).
(15) We used a CI based on the MOs of the half electron singlet; cf. M. J. S. Dewar and C. E. Doubleday, *J. Am. Chem. Soc.*, to be published.
(16) A. W. Salotto and L. Burnelle, *J. Chem. Phys.*, **52**, 2936 (1970).
(17) M. J. S. Dewar, S. Olivella, and H. S. Rzepa, *Chem. Phys. Lett.*, **47**, 80 (1977).
(18) A. J. Dorney, A. R. Hoy, and I. M. Mills, *J. Mol. Spectrosc.*, **45**, 253 (1973).
(19) B. I. Swanson and R. S. Ottinger, Quantum Chemistry Progran Exchange No. 208.
(20) S. Konaka, Y. Murata, K. Kuchitsu, and Y. Morion, *Bull. Chem. Soc. Jpn.*, **33**, 1134 (1966).
(21) L. H. Jones, "Inorganic Vibrational Spectroscopy", Vol. 1, Marcel Dekker, New York, N.Y., 1971.
(22) J. B. Milne and A. Ruoff, *J. Mol. Spectrosc.*, **6**, 472 (1961).
(23) R. K. Thomas and H. W. Thompson, *Proc. R. Soc. London, Ser. A*, **314**, 329 (1970).
(24) J. L. Duncan, *J. Mol. Spectrosc.*, **22**, 247 (1967).
(25) S. G. W. Ginn, D. Johansen, and J. Overend, *J. Mol. Spectrosc.*, **36**, 448 (1970).
(26) C. W. Brown and J. Overend, *Can. J. Phys.*, **46**, 977 (1968).
(27) I. W. Levin and S. Abramowitz, *J. Chem. Phys.*, **43**, 4213 (1965).
(28) K. Hirata and Y. Morino, as reported in T. Shimanouchi, I. Nakagawa, J. Hiraishi, and M. Ishii, *J. Mol. Spectrosc.*, **19**, 78 (1968).
(29) W. F. Edgell and R. E. Moynihan, *J. Chem. Phys.*, **27**, 155 (1957); **45**, 1205 (1966).
(30) N. Dreska, K. N. Rao, and L. H. Jones, *J. Mol. Spectrosc.*, **18**, 404 (1965).
(31) D. R. Stull and H. Prophet et al., "JANAF Thermochemical Tables", 2nd ed, NSRDS-NBS37, U.S. Government Printing Office, Washington, D.C., 1971.
(32) W. Moffit, *Proc. R. Soc. London*, **200**, 409 (1950).
(33) J. C. D. Brand, C. di Lauro, and V. T. Jones, *J. Am. Chem. Soc.*, **92**, 6096 (1970).
(34) J. H. D. Eland and C. J. Danby, *Int. J. Mass Spectrom. Ion Phys.*, 1, 111 (1968).
(35) R. G. Wycoff, "Crystal Structures", Vol. 3, 2nd ed, Interscience, New York, N.Y., 1965.

Chemical Applications of Group Theory and Topology. 7. A Graph-Theoretical Interpretation of the Bonding Topology in Polyhedral Boranes, Carboranes, and Metal Clusters[1c]

R. B. King*[1a] and D. H. Rouvray[1b]

Contribution from the Department of Chemistry, University of Georgia, Athens, Georgia, 30602, and the Chemistry Department, University of the Witwatersrand, 2001 Johannesburg, South Africa.

Received October 25, 1976

Abstract: The bonding topology in three-dimensional closed deltahedral systems such as the cage boranes, carboranes, and some metal clusters can be analyzed completely analogously to that in delocalized two-dimensional polygonal systems such as benzene by algebraic graph-theoretical methods. Such methods make use of the complete graphs K_n rather than the cyclic graphs C_n to represent the interactions between the unique internal orbitals of the vertex atoms. This analysis provides a theoretical basis for the stability of closed deltahedral systems with n vertices and $2n + 2$ skeletal electrons. The anomaly of tetrahedral systems in requiring 12 rather than 10 skeletal electrons appears to be a consequence of edge-localized bonding in the tetrahedron arising from the degree three of all of its vertices. This graph-theoretical analysis of bonding topology can also be applied to the electron-rich nido systems with one hole, n vertices, and $2n + 4$ skeletal electrons as well as to less delocalized systems with even more skeletal electrons and holes. Electron-poor polyhedral cluster systems with n vertices and less than $2n + 2$ skeletal electrons form deltahedra with one or more capped faces and normally require transition metals, rather than boron or carbon, at the vertices of the capped faces. Puncture or excision of closed deltahedra to form electron-rich open polyhedra with one or more holes may be considered as opposite or dual to the capping of closed deltahedra to form electron-poor larger deltahedra with tetrahedral chambers.

I. Introduction

One of the most interesting and significant developments in inorganic chemistry during the past two decades has been the discovery of boron cage compounds exhibiting unusually high stability and low chemical reactivity such as the dianions[2,3] $B_nH_n^{2-}$ $(6 \leq n \leq 12)$, and the carboranes[4] $C_2B_{n-2}H_n$ $(5 \leq n \leq 12)$. Some LCAO-MO calculations by the extended Hückel method on these systems in 1962 shortly after their discovery[5] gave results consistent with the presence of $n + 1$ skeletal bonding orbitals corresponding to $2n + 2$ skeletal bonding electrons in closed polyhedral systems with n vertices and only triangular faces. Subsequent work[6-9] has provided additional evidence for the particularly high stability of closed polyhedral systems with n vertices and $2n + 2$ skeletal electrons. A further development of this more recent work[6,8,9] has been a demonstration of the close analogies between the skeletal bonding in boron cage compounds and that in metal clusters,[10] particularly those of high nuclearity.[11]

This paper presents the first analysis of the bonding topology in these triangulated polyhedral systems using algebraic graph theory.[12] Our new treatment of polyhedral boranes and metal clusters generates directly the $n + 1$ skeletal bonding orbitals in closed polyhedral systems with n vertices. For this reason, we believe that this graph-theoretical analysis will be of con-